Calibration of Multi-Channel Spaceborne SAR – Challenges and Strategies –

Marwan Younis, Christopher Laux, Noora Al-Kahachi, Paco López-Dekker, Gerhard Krieger, and Alberto Moreira
German Aerospace Center (DLR), Oberpfaffenhofen, Germany

Abstract

Instrument calibration has ever been essential to synthetic aperture radar. This paper reviews the calibration functionality of current state-of-the-art spaceborne SAR and then proceeds to suggest calibration strategies for future SAR systems. These systems will incorporate multi-channel digital beamforming capabilities which offer new opportunities but also challenges for digital calibration. At the same time, the increased complexity of instrument calibration can not be extrapolated to future systems. This requires a reconsideration of the calibration strategy for spaceborne SAR. The paper is seen as a step in this direction.

1 Spaceborne SAR Calibration

Current SAR systems have reached a high maturity in exploiting calibration [1]. Instrument deviation from the ideal operation, long and short time drifts, mismatch and coupling between the RF paths are measured. In addition, external effects such as atmospheric and ionospheric disturbances are characterized. The purpose of calibration is to minimize the impact of the known errors. This is achieved by *i)* tuning the instrument in real-time to compensate the errors; *ii)* subsequently modifying the instrument settings to remove errors based on the analysis of the calibration data on ground; and *iii)* mitigating the effect of known errors (without removing the error source) by considering it within the SAR data processing.

1.1 Internal Instrument Calibration

Dedicated calibration pulses are injected into the signal paths using elaborate cal-networks [2]. To guarantee the required accuracies in the order of fractions of a dB, the cal-networks are characterized on ground to minimize the measurement uncertainty. Various calibration loops are implemented to measure the transmit and receive paths as well as the central electronics. This enables constructing a replica, i.e. a reference signal, affected by the characteristics of the SAR signal path.

A typical Transmit/Receive Module (TRM) architecture is shown in **Figure 1** where the numbers are associated to the different functionality of the respective hardware blocks. In order to characterize the Rx path of ①, a known reference signal is injected into the receive path using cal-network ③ and coupler ②. The Tx path of ① is measured by using the same coupler to extract a small fraction of the signal which is routed to the receiver through the cal-network ③. The cal-network itself needs to be accurately characterized on ground, so that its distortion is known. Neither the polarization switch nor antenna itself ④ are part of the calibration loop. Their error contribution is thus not measured! Finally, the cal-signals

of all the TRMs are combined in ⑤. It is thus only the sum of cal-signals which is available, this is equivalent to a boreside beam and does not represent the actual instrument state [3]. Due to the large number of TRMs it is not possible to measure a single TRM by switching off all modules except the one being characterized. Instead elaborate pseudo noise sequences are used [4].
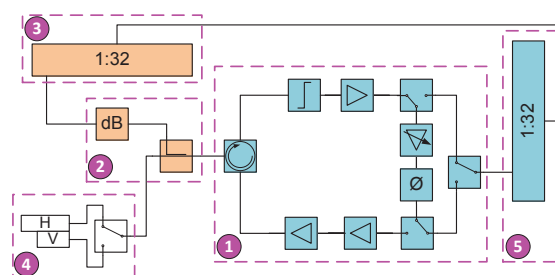

Figure 1: An example Tx/Rx-Module (TRM) architecture including the blocks for calibration.

1.2 Internal T/R-Module Correction

Nearly all current SAR systems offer multiple operation modes, which are realized by steering and shaping the transmit and receive beams. For this, several hundred TRMs are used to set the phase and amplitude for the elements of the antenna. The instrument and antenna pattern stability is achieved by engineering self calibrating procedures internal to the TRMs, i.e. within block ① of Figure 1. This is achieved by multidimensional correction tables (temperature vs. power vs. polarization vs. Rx/Tx) obtained through lengthy on-ground characterization measurements. These tables are stored in the memory of each TRM and typically applied in an autonomous manner. At the same time, the TRMs are also part of the calibration loops (cf. previous section).

1.3 External Calibration

External calibration is carried out with the SAR system operating in space and complements the internal calibration. Both active (transponders and receivers) and passive (corner reflectors) cal-targets are positioned within the swath, measured during dedicated campaigns, and within the operational phase. This enables the verification of the antenna patterns shape, power levels, and instrument stability, which leads to the radiometric calibration. The Tx patterns are obtained through direct measurement, while the Rx pattern parameters are estimated from the SAR image. Further, the high reflectivity of the cal-targets enables an accurate system impulse response measurement. The response of the calibration targets must be stronger than the surrounding clutter; as such the measured power levels might not be representative of typical SAR scenes. To measure the small deviations associated to the high SAR accuracy, targets of even higher accuracy need to be fabricated, which leads to calibration targets which include internal calibration networks.

2 Multi-Channel SAR Calibration

Most SAR systems currently in orbit are based on TRM technologies. It is not forseen that this will change in the near future[1]. However, there is a trend towards digital multi-channel systems, as can be seen for some existing sensors. For example TERRASAR-X offers two channel capabilities as a by-product of the redundancy concept; RADARSAT-2 has along-track capabilities through two channels; and ALOS-2 improves the azimuth resolution by utilizing two channels. This step towards multi-channel SAR marks a paradigm change for the next two decades! Still, the calibration strategies foreseen for future multi-channel SAR are not being adapted to the particularities of the new systems.

However, current instrument calibration designs do not consider advances in other related calibration areas. One of these fields is polarimetric calibration which was boosted 20 years ago as documented by a series of excellent publications [5]. Today polarimetric calibration is, to a large extent, based on comparing processed SAR data to both known point target responses and model statistics of natural distributed targets. The fact that statistical quantities of the sensor's data may be used for calibration is mostly ignored in the conception of instrument calibration strategies. Realizing that polarimetric SAR is indeed a two-channel SAR motivates applying the concepts and ideas of polarimetric error correction to future multi-channel SAR. Similar argumentation applies to interferometry, which is sensitive to smallest phase errors. TANDEM-X for example, requires a phase knowledge accuracy of less than $1°$ [6]. To some extent this can be achieved by co-registration techniques [7] which can correct even the oscillator phase noise. This can be understood as an external calibration technique which does not utilize dedicated cal-targets or cal-signals.

2.1 Multi-Azimuth Receive System

A simplified but typical receive architecture of Multiple Azimuth Channels (MACs) is shown in **Figure 2**. Depending on the realization, two or more azimuth sub-arrays are amplified and combined before being digitized. In this case, the amplifiers are required to be highly (phase) stable for proper summation. Here, injecting a cal-tone to measure the error is useless, since it can not reconstruct the signals before combination. The only potential advantage of a cal-tone is to know the error and for constructing the replica.
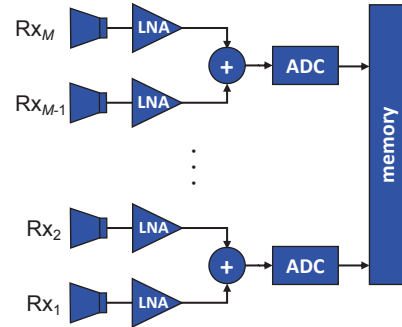

Figure 2: Schematic architecture of Multi-Azimuth Channels (MACs) receive chain.

When utilizing MACs the data stream of each azimuth channel will be stored in on-board memory (usually after some data compression) and later down-linked to the ground for processing. Extracting the redundancies which occur in the case of oversampling is too computationally extensive to be carried out on-board.

Various methods exist for on-ground processing. Since the signals of the individual channels are ambiguous, some kind of Doppler spectrum reconstruction is necessary [8]. This can be understood as null steering (in Doppler frequency domain) which is highly sensitive to the relative phases between the channels. Thus, here the challenge is inter-channel calibration (or channel balancing) and an accurate knowledge of the complex sub-array radiating patterns, which need to be considered in the reconstruction. Multiple publications are available on azimuth channel error corrections [9, 10, 11]. Since this is carried out on-ground, it can use computational intensive algorithms to determine data statistics as well as iterative error correction algorithms.

2.1.1 Multi-Elevation Receive System

The situation is rather different for the case of multiple digital channels in elevation (cf. **Figure 3**). The DBF technique used here is known as SCORE and consists of a time varying weighted digital combination of signals in elevation for redundancy (and data) reduction [12]. This technique is vulnerable to phase errors of the individual channels. To understand this, consider a phase error resulting in a constant beam pointing error. Clearly

---

[1]An exception may be Ka-band and higher frequency SAR systems, where TRM technology is disadvantageous in terms of power generation.

the beam would not "see" the ground echo resulting in a noise-only received signal. A high accuracy requirement also applies to the time varying weights, but here the complex multiplication is carried out in the digital domain, by which the errors can be made sufficiently small through proper design. Some SAR operation modes require nulling techniques in elevation, but this is not the most common case.
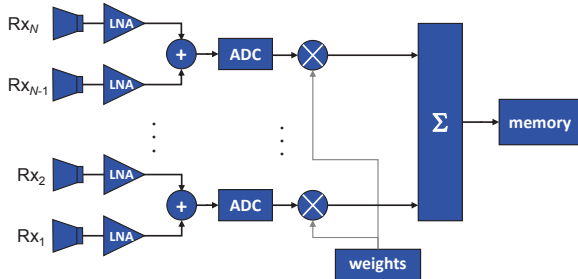

Figure 3: Schematic architecture of as used for SCan-On-REceive (SCORE) operation.

In elevation, the calibration procedures must run in real time on-board the instrument. Thus conventional calibration with signal injection and summation is inherently incapable to correct the errors. One approach is to analyze the calibration signal on-board to extract the phase and amplitude offsets between the channels; then the digital weights can be re-computed to mitigate these errors.

An alternative approach which is proposed here is data driven, meaning that the error correction values are derived from the (raw) SAR data. Various algorithms are available in literature; for example [13] uses an approach based on maximizing the contrast (the paper also gives a good overview of existing cal-methods) and [14] which uses the spatial correlation between antenna elements. Data driven calibration is attractive, because it operates independently of whether the components causing the errors are included in the calibration path or not. In some cases the data correction is inherent to the calibration algorithm, i.e. the errors are compensated without explicitly being "known" to the algorithm. Further, effects such as the power loss in case of unknown DEM and the pulse extension loss (cf. [15]) can be corrected.

# 3 Data Driven Calibration Performance Example

In this section the application of a data driven calibration algorithm based on the correlation between antenna elements is shown. It is based on a method developed by ATTIA & STEINBERG in [14] which basically shows that the correlation between the signals of any two antenna elements (spatial correlation) depends only on the separation between the two elements. The underlying model assumes the signals to originate from non-coherent scatterers, i.e. the typical raw echo signal (clutter) of a radar imaging a distributed scene. Most data driven calibration techniques are suitable for calibrating slowly varying er-

rors. This is because of the computational load and the number of independent measurements needed. This is also true for the technique described here, which is understood to compensate a slow instrument drift.

The spatial correlation function is computed based on an implementation of [14] for a Sentinel-1A follow-on like SAR employing a $12.8\,\text{m} \times 1.2\,\text{m}$ (length x height) antenna consisting of 8×14 channels in azimuth and elevation, respectively. **Figure 4a** shows the magnitude and phase, respectively, of the spatial correlation in elevation versus the distance normalized to the wavelength; the markers indicate the position of antenna elements. No ambiguities are considered. Typically only the signals of adjacent elements can be utilized for calibration, because of the rapid drop in the correlation; here however we note the slowly dropping correlation amplitude which indicates that multiple elements may be utilized for the calibration as long as the correlation between the first and last element is still high enough. The reason for this high correlation between multiple elements is that the data space of the individual elements is not filled (cf. [16]). The reason for that is as follows: At any time instance the echo signal is received from a small angular segment corresponding to the transmit pulse extent on the ground (here approximately $1.1°$, see [15]), while each element sees a much larger angular segment (nearly $35°$). The fact that SCORE is utilized reducing the data rate without a loss of information evidences this.
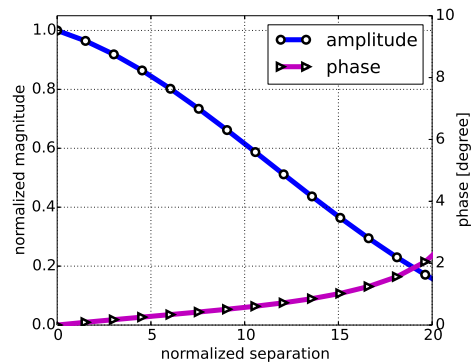
(a) correlation of elevation elements
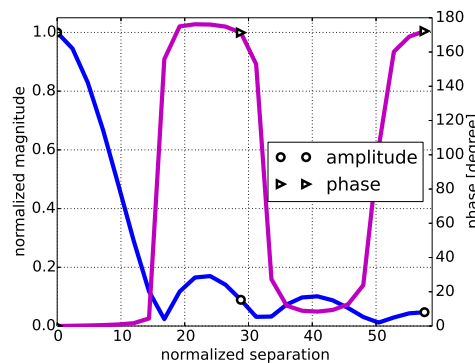
(b) correlation of azimuth elements

Figure 4: The amplitude and phase of the normalized spatial autocorrelation function. Note that the scale is different for the upper and lower figure.

The spatial correlation function for the azimuth channels is shown in **Figure 4b**. Here the spatial spectrum occupied by the signal is in the same order of magnitude as that of the elevation beam, however, because the azimuth element size is much larger (approximately 28λ) the separation becomes larger and the actual correlation between adjacent elements is decreased.

The higher the correlation the more is the *a priori* knowledge of the phase difference between the elements. This is also visualized in **Figure 5** which represents the results of a simulation where random uniform phase errors have been introduced to the signals received by the antenna elements in addition to an additive Gaussian noise of $10\,\text{dB}$ signal-to-noise ratio at each element. A qualitative assessment of the calibration accuracy is shown in **Figure 5** which represents the residual phase errors matrix in a logarithmic scale after utilizing the procedure in [14] to correct for the phase errors assuming that 500 independent measurements are available (e.g. different range gates). The value on the abscissa represents the distance between the antenna elements whose signals are being correlated; The left most values (first column of the residual phase error matrix) results from comparing pairs of adjacent elements, next every element is correlated to the one following its neighbor (second column of the matrix) and so on. The residual error is very small when the correlation between adjacent elements is used, however increasing the separation reduces the correlation and by this increases the residual error as seen when moving to the upper right corner of the image. A quantitative analysis of the residual error shows that its value is below $1°$ for separations up to six elements!
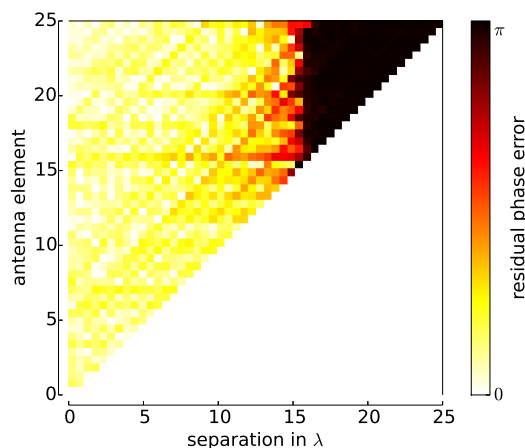

Figure 5: Representation of the residual error matrix where the color coding corresponds to a logarithmic measure of the phase error.

References

[1] A. Freeman, "SAR calibration: An overview," *IEEE Transactions on Geoscience and Remote Sensing*, vol. 30, no. 6, pp. 1107–1121, Nov. 1992.

[2] B. Bräutigam, J. Gonzalez, M. Schwerdt, and M. Bachmann, "TerraSAR-X instrument calibration results and extension for TanDEM-X," *IEEE Transactions on Geoscience and Remote Sensing*, vol. 48, no. 2, pp. 702–715, Feb. 2010.

[3] E. Makhoul, A. Broquetas, P. López-Dekker, J. Closa, and P. Saameno, "Evaluation of the internal calibration methodologies for spaceborne synthetic aperture radar with active phased array antennas," *IEEE Journal on Selected Topics in Applied Earth Observation and Remote Sensing*, vol. 5, pp. 909–918, June 2012.

[4] B. Bräutigam, M. Schwerdt, M. Bachmann, and M. Stangl, "Individual T/R module characterisation of the TerraSAR-X active phased array antenna by calibration pulse sequences with orthogonal codes," in *Proc. Int. Geoscience and Remote Sensing Symposium IGARSS'2007*, Barcelona, Spain, July 2007.

[5] J. van Zyl, "Calibration of polarimetric radar images using only image parameters and trihedral corner reflector responses," *IEEE Transactions on Geoscience and Remote Sensing*, vol. 28, no. 3, 1990.

[6] G. Krieger, A. Moreira, H. Fiedler, I. Hajnsek, M. Werner, M. Younis, and M. Zink, "TanDEM-X: A satellite formation for high resolution SAR interferometry," *IEEE Transactions on Geoscience and Remote Sensing*, vol. 45, no. 11, pp. 3317–3341, Nov. 2007.

[7] M. Rodriguez-Cassola, P. Prats, D. Schulze, N. Tous-Ramon, U. Steinbrecher, L. Marotti, M. Nannini, M. Younis, P. López-Dekker, M. Zink, A. Reigber, G. Krieger, and A. Moreirea, "First bistatic spaceborne SAR experiments with TanDEM-X," *IEEE Geoscience and Remote Sensing Letters*, vol. 9, no. 1, pp. 33–37, Jan. 2012.

[8] G. Krieger, N. Gebert, and A. Moreira, "Unambiguous SAR signal reconstruction from non-uniform displaced phase centre sampling," *IEEE Geoscience and Remote Sensing Letters*, vol. 1, no. 4, pp. 260–264, Oct. 2004.

[9] C. Gierull, "Digital channel balancing of along-track interferometric SAR data," DRDC Ottawa, Technical Memorandum DRDC-OTTAWA-TM-2003-024, Mar. 2003.

[10] T. Yang, Z. Li, Y. Liu, and Z. Bao, "Channel error estimation methods for multichannel SAR systems in azimuth," *IEEE Geoscience and Remote Sensing Letters*, vol. 10, no. 3, May 2013.

[11] M. Gabele, B. Bräutigam, D. Schulze, U. Steinbrecher, N. Tous-Ramon, and M. Younis, "Fore and aft channel reconstruction in the TerraSAR-X dual receive antenna mode," *IEEE Transactions on Geoscience and Remote Sensing*, vol. 48, no. 2, pp. 795–806, Feb. 2010.

[12] M. Süß, B. Grafmüller, and R. Zahn, "A novel high resolution, wide swath SAR," in *Proc. Int. Geoscience and Remote Sensing Symposium IGARSS'01*, vol. 3, 2001, pp. 1013–1015.

[13] G. Farquharson, P. López-Dekker, and S. J. Fraiser, "Contrast-based phase calibration for remote sensing systems with digital beamforming antennas," *IEEE Transactions on Geoscience and Remote Sensing*, vol. 51, pp. 1744–1754, Mar. 2013.

[14] E. H. Attia and B. D. Steinberg, "Self-cohering large antenna arrays using the spatial correlation properties of radar clutter," *IEEE Transactions on Antennas and Propagation*, vol. 37, pp. 30–38, Jan. 1989.

[15] M. Younis, S. Huber, A. Patyuchenko, F. Bordoni, and G. Krieger, "Performance comparison of reflector- and planar-antenna based digital beamforming SAR," *Int. Journal of Antennas and Propagation*, vol. 2009, June 2009. [Online]. Available: http://www.hindawi.com/journals/ijap/2009

[16] G. Krieger, N. Gebert, and A. Moreira, "Multidimensional waveform encoding: A new digital beamforming technique for synthetic aperture radar remote sensing," *IEEE Transactions on Geoscience and Remote Sensing*, vol. 46, no. 1, pp. 31–46, Jan. 2008.